
MENTOR: Guiding Hierarchical Reinforcement Learning with Human Feedback and Dynamic Distance Constraint

Xinglin Zhou¹

Yifu Yuan²

Shaofu Yang¹

Jianye Hao²

¹School of computer science and engineering, Southeast University, Nanjing, Jiangsu, China

²College of Intelligence and Computing, Tianjing University, Tianjing, China

Abstract

Hierarchical reinforcement learning (HRL) provides a promising solution for complex tasks with sparse rewards of intelligent agents, which uses a hierarchical framework that divides tasks into subgoals and completes them sequentially. However, current methods struggle to find suitable subgoals for ensuring a stable learning process. Without additional guidance, it is impractical to rely solely on exploration or heuristics methods to determine subgoals in a large goal space. To address the issue, We propose a general hierarchical reinforcement learning framework incorporating human feedback and dynamic distance constraints (MENTOR). MENTOR acts as a “mentor”, incorporating human feedback into high-level policy learning, to find better subgoals. As for low-level policy, MENTOR designs a dual policy for exploration-exploitation decoupling respectively to stabilize the training. Furthermore, although humans can simply break down tasks into subgoals to guide the right learning direction, subgoals that are too difficult or too easy can still hinder downstream learning efficiency. We propose the Dynamic Distance Constraint (DDC) mechanism dynamically adjusting the space of optional subgoals. Thus MENTOR can generate subgoals matching the low-level policy learning process from easy to hard. Extensive experiments demonstrate that MENTOR uses a small amount of human feedback to achieve significant improvement in complex tasks with sparse rewards.

challenging exploration, and unstable training. In recent years, several approaches have been proposed to relieve these issues, including goal-conditional reinforcement learning [Andrychowicz et al., 2017], curiosity-driven exploration [Burda et al., 2018] and hierarchical reinforcement learning [Levy et al., 2017, Nachum et al., 2018, Hutsebaut-Buysse et al., 2022].

HRL is effective for long-horizon tasks with sparse rewards, as it divides these into more manageable subgoals, easing the issues of challenging exploration and unstable training. However, there are two difficulties in the practical application of HRL. (1) Generating instructive subgoals. Several studies have focused on proposing methods to address the challenges associated with generating efficient subgoals for guiding low-level policy. These methods involve both manual design approaches [Dietterich, 2000, Parr and Russell, 1997] and automatic generation [Zhang et al., 2022, Eysenbach et al., 2018, Park et al., 2023, Hutsebaut-Buysse et al., 2022]. However, each has drawbacks: manual design is costly and challenging to solve complex tasks [Ahn et al., 2022], while automatic generation requires extensive resources to search the entire state space [Campos et al., 2020]. (2) Completing subgoals efficiently. As for low-level, hindsight relabeling [Andrychowicz et al., 2017] modifies subgoals to convert failed transitions into successes but lacks exploratory capabilities. Curiosity-driven methods like RND prevent state revisitation [Bougie and Ichise, 2022] but can destabilize training due to reward exploration bonuses, especially with sparse rewards. At the high-level, previous research primarily focused on modifying subgoals to address non-stationarity in high-level policy updates when low-level actions fail to achieve these subgoals [Levy et al., 2017, Nachum et al., 2018]. However, these adjustments mainly address non-stationarity resulting from failures without ensuring low-level success in subgoal achievement. Levy et al. [2017] suggest penalizing high-level policies, but such penalties are ineffective if the low-level always fails.

In this paper, we introduce a new framework named MENTOR, incorporating human feedback into high-level policy

1 INTRODUCTION

The problem of sparse reward is consistently challenging in the domain of reinforcement learning (RL) [Reddy et al., 2019, Vecerik et al., 2017], attributing to two main factors:

learning to find better subgoals. To guide an agent in exploration, MENTOR incorporates human guidance for subgoal generation at the high-level. While humans may not accomplish complex tasks, they can give directions. Reinforcement Learning from Human Feedback (RLHF) is a technique that learns human preferences through binary comparisons of subgoals, offering directional guidance. Therefore, the high-level can receive instruction, resulting in dual advantages between HRL and RLHF.

To enable an agent to quickly complete subgoals, one low-level policy struggles to accomplish subgoals while introducing curiosity-driven exploration. Hence, we introduce Exploration-Exploitation Decoupling (EED), which uses one policy to explore while the other policy learns from the experience of the exploring policy to stabilize the training. As for the high-level, humans can provide direction, yet subgoals might not align with low-level capabilities because they may be too difficult or too easy. For cooperation between the high-level and low-level, a method called Dynamic Distance Constraint is proposed. It uses distance as a measure of subgoal difficulty and restricts the high-level subgoal space to align subgoal difficulty with low-level capabilities. We summarize the main contributions as follows:

- We propose MENTOR, leveraging human feedback to guide the subgoal direction and Exploration-Exploitation Decoupling to simultaneously realize exploration and exploitation in subgoal attainment.
- We introduce Dynamic Distance Constraint, dynamic aligning the subgoal difficulty to the capabilities of the low-level policy.
- We demonstrate that MENTOR outperforms other baselines in accomplishing tasks with sparse rewards across various domains.

2 RELATED WORK

2.1 HIERARCHICAL REINFORCEMENT LEARNING

In the field of HRL, identifying meaningful subgoals within long-horizon tasks has been extensive research. This includes studies on options [Bacon et al., 2017, Harb et al., 2018, Bagaria and Konidaris, 2019], goals [Andrychowicz et al., 2017, Schaul et al., 2015, Levy et al., 2017] and skills [Eysenbach et al., 2018, Sharma et al., 2019, Park et al., 2023]. Manual-designed subgoals are costly and challenging for complex tasks [Ahn et al., 2022]. Automatic learning of meaningful subgoals without any guidance from an external expert is a significant challenge [Jinnai et al., 2019]. CSD [Park et al., 2023] aims to discover latent skills via mutual-information maximization. However, combining meaningful skills into task completion is a continuous challenge. HAC [Levy et al., 2017] addresses the challenges of

sparse reward and non-stationarity at high-levels through the utilization of hindsight action transitions and hindsight goal transitions. HIRO [Nachum et al., 2018] employs a model to generate a new high-level action to rectify the high-level transitions. However, Both HAC and HIRO focus on solving non-stationary problems but fall short in task decomposition. Our research incorporates human guidance and DDC to identify appropriate task decomposition. Human insights provide subgoal direction; DDC limits subgoal difficulty.

2.2 REINFORCEMENT LEARNING FROM HUMAN FEEDBACK

The surge in popularity of ChatGPT [Brown et al., 2020, Ouyang et al., 2022] has significantly boosted the recognition of RLHF in recent times. RLHF is an effective technique that can expedite AI training and bolster AI capabilities through the utilization of human feedback [Lee et al., 2021a,b, Park et al., 2022]. RLHF learns reward functions from pairwise comparison and ranking based on human preference [Lee et al., 2021a, Shah et al., 2016, Ouyang et al., 2022, Saha and Krishnamurthy, 2022]. Human intuition and experience can be incorporated as guidance in high-level decision-making, particularly in setting subgoals within the HRL framework [Bougie and Ichise, 2022]. Nevertheless, humans may struggle to offer immediate guidance that corresponds with the agent’s capabilities.

3 PRELIMINARY

3.1 PROBLEM SETTING

In this work, we consider high-level actions as goal states and provide rewards to the low-level policy for executing actions that result in resembling the desired goal. We define Markov Decision Process with a set of goals, characterized by the tuple $\langle \mathcal{S}, \mathcal{G}, \mathcal{A}, P, R, \gamma \rangle$, in which \mathcal{S} is the set of states; \mathcal{G} is a set of goals, which is equivalent to the set \mathcal{S} . \mathcal{A} is the set of actions; $P(s'|s, a)$ is the transition probability function; $R(r|s', g)$ is the reward function; γ is the discount rate $\in [0, 1)$. We can define the reward function $r_g(s) = \mathbb{1}(\|g - s\|_2 < \epsilon)$, which ϵ is a distance threshold determining contact. The problem of goal-conditioned task can be defined mathematically as $\pi \leftarrow \arg \max_{\pi} \mathbb{E}_{\mathcal{T} \sim \pi(s, g)} [\sum_{t=1}^H \lambda^t r_g(s_t)]$.

3.2 HINDSIGHT RELABELLING

Hindsight relabelling Andrychowicz et al. [2017] addresses sparse reward in GCRL by redefining failed transitions as successful transitions, thus generating positive rewards. Specifically, for a failed transition $(s_t, a_t, r_t, s_{t+1}, g)$ with $r_t = \mathbb{1}(\|g_t - s_{t+1}\|_2 < \epsilon) = 0$, it resets the transition as

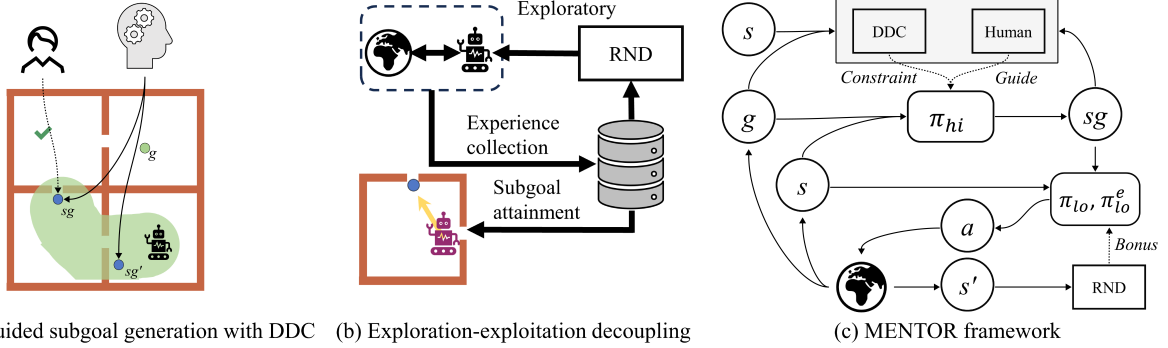


Figure 1: (a) The high-level policy selects subgoals with DDC (shades of green), and human guides by comparing these subgoals. (b) The low-level decouples exploration and exploitation through two policies, one policy explores the environment and the other learns from the experience of exploration. (c) Diagrammatic representation of MENTOR framework.

$(s_t, a_t, 1, s_{t+1}, g')$ with goal $g' = s_{t+1}$. By utilizing this new transition, it becomes possible to train an off-policy RL algorithm with more positive rewards.

3.3 CURIOSITY-DRIVEN EXPLORATION

Intrinsic motivation has been utilized to encourage agents to learn about their surroundings, even when extrinsic rewards are scarce [Bellemare et al., 2016, Pathak et al., 2017, Burda et al., 2018]. In this framework, RND Burda et al. [2018] serves as the intrinsic reward. RND consists of two neural networks, represented as $f : \mathcal{S} \rightarrow \mathbb{R}^k$ and $\hat{f} : \mathcal{S} \rightarrow \mathbb{R}^k$, which are both randomly initialized and capable of transforming observations into embeddings. By keeping one network fixed and training the other network to minimize prediction distance, the intrinsic reward is formulated as $r_{rnd}(s_t) = \|\hat{f}(s_t) - f(s_t)\|^2$. This intrinsic reward encourages the agent to visit novel states, as it will be higher in regions of the state space that the predictor network finds difficult to approximate, thus fostering exploration in the learning process.

4 METHODOLOGY

As shown in Figure 1, we propose MENTOR, utilizing a small amount of noisy human feedback to address the challenge of generating complex subgoals at the high-level. At the low-level, it decouples exploration and exploitation, solving the instability associated with curiosity-driven exploration. Additionally, we introduce DDC, a technique to constrain the range of high-level subgoals, aligning their difficulty with the low-level capabilities. MENTOR enables the high-level policy to set subgoals, while the low-level efficiently achieves them, facilitating rapid and stable learning. For detailed implementation, please see Appendix A.

4.1 FRAMEWORK FORMALIZATION

We briefly review here to introduce notation. The framework consists of four neural networks: high-level policy $\pi_{hi} : \mathcal{S} \times \mathcal{G} \rightarrow \mathcal{G}$, low-level policy $\pi_{lo} : \mathcal{S} \times \mathcal{G} \rightarrow \mathcal{A}$, reward model learned by human feedback $r_{hf} : \mathcal{S} \times \mathcal{G} \times \mathcal{G} \rightarrow [0, 1]$ and RND model $f_{rnd} : \mathcal{S} \rightarrow [0, 1]$ with parameters $\theta_{hi}, \theta_{lo}, \theta_{hf}$ and θ_{rnd} respectively. In the following, we will explain how the high-level incorporates human guidance and the low-level stabilizes the training process.

High-level Policy. Subgoal generation poses a significant challenge, with manual setup being costly and difficult, while automatic methods demand extensive computational resources to explore the state space. High-level subgoal generation requires macro, abstract, and generalized guidance, closely related to human preferences. RLHF offers human preferences through sample comparisons. Applied to HRL, it addresses the challenge of defining subgoals, while HRL mitigates the issue of vague and noisy preferences in RLHF, creating a mutual benefit for both HRL and RLHF.

RLHF uses pairwise comparison to train a reward model which can be used as the reward function for the high-level policy. The training process consists of 1) extracting pairs (s_1, sg_1, g) and (s_2, sg_2, g) from the high-level replay buffer. 2) Human annotators provide pairwise feedback v which 0 prefers (s_1, sg_1, g) , and 1 prefers (s_2, sg_2, g) . Preference can be assessed by the distance to the environment goal g . 3) After collecting the feedback dataset into the reward model buffer B_{hf} , we can train the reward model r_{hf} by optimizing a modified Bradley-Terry objective [Bradley and Terry, 1952]. We define the possibility that human prefers (s_1, sg_1, g) to (s_2, sg_2, g) :

$$P[(s_1, sg_1) \succ (s_2, sg_2) | g] = \frac{\exp(r_{hf}(s_1, sg_1, g))}{\sum_{i=1}^2 \exp(r_{hf}(s_i, sg_i, g))}. \quad (1)$$

Then the modified Bradley-Terry objective is as follows:

$$\begin{aligned} \max_{r_{h,f}} \mathbb{E}_{(s_1, sg_2, s_1, sg_2, g, v) \sim B_{h,f}} & \\ [v \log(P[(s_1, sg_1) \succ (s_2, sg_2)|g]) + & \quad (2) \\ (1 - v) \log(P[(s_2, sg_2) \succ (s_1, sg_1)|g])] & \end{aligned}$$

In optimizing the high-level policy, the high-level reward function is set to be $r_{hi} = r_{h,f}(s, sg, g)$. Nevertheless, two issues arise with this direct implementation of $r_{h,f}$. (1) Training the reward model with all off-policy data is inefficient. When the low-level policy is already capable of achieving subgoals, comparing these subgoals is unnecessary for reward model training. For the issue, we propose training the reward model with near-policy data, using (s, sg, g) pairs sampled from recent episodes. This approach focuses on the most relevant data, reducing computational and model complexity. (2) In some cases, the high-level policy may fall into a local optimum due to the lack of a pretraining step to improve the reward function by comparing more diverse samples. Therefore, it is important to encourage the high-level to explore. We introduced some exploration techniques such as RND and maximum entropy (MaxEnt) [Mei et al., 2020]. We apply MaxEnt and set $r_{hi} = r_{h,f}(s, sg, g) - \beta \cdot \mathbb{E}_{sg \sim \pi_{hi}(\cdot|s,g)} \log \pi_{hi}(sg|s, g)$. β is a small constant.

Low-level Policy. Sparse rewards hinder the low-level ability to quickly achieve subgoals. Current research employs hindsight relabelling, which limits exploration capabilities and leads to repeated exploration. Introducing RND can mitigate repeated exploration by promoting novel discoveries, though its direct implementation may result in instability. RND’s exploration incentives might lead to neglecting the task of subgoal completion. To address this issue, we propose EED, a dual policy program, consisting of an exploration policy π_{lo}^e and a base policy π_{lo} , both sharing the same data buffer. During interactions with the environment, we employ the exploration policy π_{lo}^e and store the experiences in the shared replay buffer. For policy updates, both the exploration and base policies undergo a hindsight relabelling process for relabeled transition data. Then, the exploration policy is updated using reward $r_g(s', sg) + f_{rnd}(s')$. The base policy is updated using the reward $r_g(s', sg)$. This method allows the base policy to learn from novel exploration data without conducting the exploration task, concentrating on achieving the intended subgoals.

4.2 DYNAMIC DISTANCE CONSTRAINT

As indicated in Figure 3, humans can provide direction to a target by providing preferences (indicated by the yellow curve) but do not have real-time knowledge of low-level capabilities. Thus multi-level simultaneous learning may be uncoordinated, resulting in subgoals that are too difficult or too simple. To solve this issue, we introduce the

DDC. This method limits the range of subgoals based on their distance from the current state (the variation in green shading depicted in the figure), ensuring they are achievable by the low-level policy. This is achieved through a specific formulation:

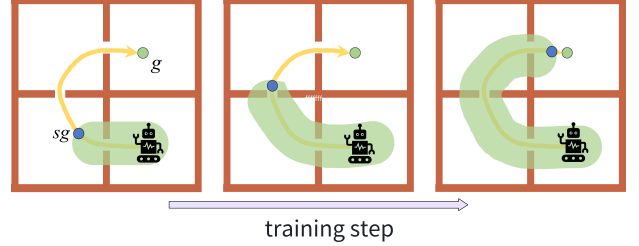


Figure 3: As the low-level capability improves, the DDC progressively relaxes, allowing the high-level to propose increasingly challenging subgoals.

$$\max_{\pi_{hi}} \mathbb{E}[r_{hi}(s, sg, g)] \quad s.t. \quad H(sg, g, k) \leq 0. \quad (3)$$

The function $H(sg, g, k) : \mathcal{G} \times \mathcal{G} \rightarrow \mathbb{R}$ is defined as $\max(d(sg, g) - k, 0)$. In this context, $d(sg, g)$ represents the distance between the subgoal sg and the goal g . The hyper-parameter k sets the subgoal space range. However, in scenarios like the Four Rooms domain, the Euclidean distance as $d(\cdot)$ may not accurately assess the difficulty of completing a task. For instance, a goal in the top right might be hard to reach despite a low Euclidean distance, indicating the need for a learned step distance measure. Therefore, in GCRL problems, it’s crucial to evaluate the step distance between unreachable subgoals and the current state. If the low-level policy fails to reach a subgoal, assigning a high distance value to these unreachable subgoals relative to the current state is essential. Neglecting to do so, high-level policies might incorrectly view challenging subgoals as easy, leading to unrealistic subgoal proposals. To tackle this issue, we recommend incorporating negative sampling into the distance model objective:

$$\begin{aligned} \min_d \frac{1}{2} \mathbb{E}_{\tau \sim \rho_{\pi_{lo}}, i \in [0, L], j \in [i, L], sg \sim \pi_{hi}(\cdot|s_0, g)} & \\ [(d(s_i, s_j) - |i - j|)^2] + \mathbb{1}(s_L \neq sg)(d(s_i, sg) - L)^2 & \quad (4) \end{aligned}$$

The objective is formulated by minimizing the expected loss across trajectories τ , sampled using the low-level policy $\rho_{\pi_{lo}}$ from recent episodes, and the goals g drawn from the environment’s distribution ρ_g . L is the length of the trajectory.

In Equation (3), optimizing is challenging because of the strict constraint. To overcome this difficulty, we utilize the relaxation technique, which allows us to establish an uncon-

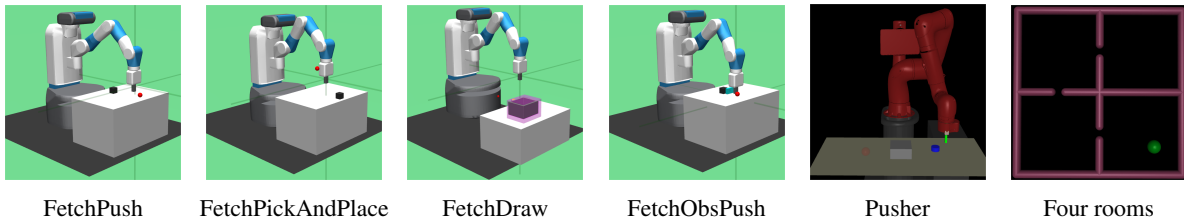


Figure 2: Experimental Domains for Evaluating MENTOR compared with baselines (see Appendix B for additional information).

strained optimization objective:

$$\max_{\pi_{hi}} \mathbb{E}[r_{hi}(s, sg) - \alpha H(sg, g, k)], \quad (5)$$

where α is a balancing coefficient to adjust the influence of reward from human guidance and distance constraint. During the training process, it is necessary to modify the hyper-parameter k to adjust the difficulty of subgoals dynamically. Hence, a fixed coefficient is inadequate to achieve the desired balance. We propose the implementation of a dynamic balancing coefficient which will be updated in real-time to maintain a balance between the rewards and distance constraints.

To effectively incorporate the adjustment into MENTOR, we need to optimize two parameters simultaneously: high-level policy θ_{hi} and balancing coefficient α , converting our maximization into a dual problem:

$$\min_{\alpha \geq 0} \max_{\pi_{hi}} \mathbb{E}[r_{hi}(s, sg, g) - \alpha H(sg, g, k)]. \quad (6)$$

The distance constraint function $H(\cdot)$ guarantees that the subgoals within a distance k . This function treats subgoals that are within the distance k as having zero effects. However, in the case of α , we want it to decrease when this constraint does not work, and increase when the high-level policies make decisions that do not satisfy this constraint. Since $H(\cdot)$ is always greater than 0 and the update gradient for α is singular, we need to eliminate the $\max(\cdot)$ function from $H(\cdot)$ to achieve automatic updates for α . We update the policy π_{hi} firstly and then coefficient α following modification for the optimization:

$$\pi_{hi}^* = \arg \max_{\pi_{hi}} \mathbb{E}[r_{hi}(s, sg, g) - \alpha H(sg, g, k)], \quad (7)$$

$$\alpha^* = \arg \min_{\alpha} \mathbb{E}[-\alpha (d(sg, g) - k)]. \quad (8)$$

After implementing DDC at the high-level, we test if the low-level can solve the subgoal, modifying the k value to tune the subgoal difficulty, ensuring multiple levels operate in coordination.

5 EXPERIMENTS

In this study, we perform a range of experiments in various domains, as depicted in Figure 2. These domains have been

widely used in previous studies [Plappert et al., 2018, Luo et al., 2023, Ghosh et al., 2019]. Through the experiments, we aim to answer the following research questions (RQs):

RQ1: How does the performance of MENTOR compare to baseline models in various domains?

RQ2: What is the impact of Dynamic Distance Constraint within MENTOR?

RQ3: What is the impact of human feedback within MENTOR?

RQ4: What insights can be gained about the individual contributions of key components in the MENTOR framework?

5.1 SETUP

Benchmarks: We select FetchPush, FetchPickAndPlace, FetchDraw, FetchObsPush, Pusher, and Four rooms as our simulation benchmarks, widely used in research [Andrychowicz et al., 2017, Ghosh et al., 2019, Bougie and Ichise, 2022]. As illustrated, the first five domains involve long-horizon manipulation tasks, while Four rooms focuses on 2D navigation.

Baselines: We have incorporated various learning methods in our baseline implementation, including techniques from HRL, RLHF, RND, dynamic distance learning, and hindsight relabelling. For further details, please see Appendix C.

- **PEBBLE** is a RL framework that incorporates human preferences into policy learning [Lee et al., 2021a].
- **HhP** applies non-expert human feedback guiding in the high-level structure and RND bonus in the low-level [Bougie and Ichise, 2022]. We implement this baseline together with hindsight relabelling for fast Learning.
- **HER** is a classical RL strategy that uses hindsight relabeling Andrychowicz et al. [2017].
- **DDL (Dynamic Distance Learning)** learns distance models. The model is utilized to train goal achievement by setting the reward as the negative distance between states and goals. The implementation follows Hartikainen et al. [2019].

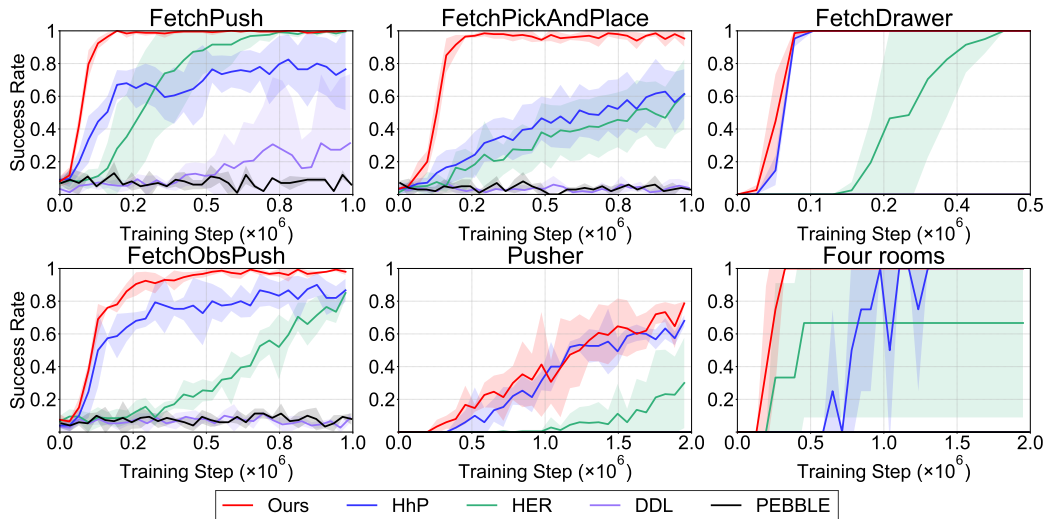


Figure 4: Graphical representation of the success rates for MENTOR in comparison to other baseline methods across different benchmarks on five random seeds. Within the domain of Four rooms, the curve behaves non-smoothly because the starting point and the goal are fixed. Any curves that are not visible in the graph, indicate a zero success rate throughout the trials. These results are aggregated from an average of five individual runs. Additionally, the shaded areas surrounding each curve represent the standard deviation.

5.2 EVALUATING MENTOR’S PERFORMANCE AGAINST BASELINES (RQ1)

In our experiments across six domains, we find that MENTOR excels in learning speed and subgoal attainment as evidenced in Figure 4. This assessment uses five random seeds and is evaluated over 50 tests. As can be seen from DDL and PEBBLE curves, DDL and PEBBLE rarely learn effectively in complex GCRL environments (effective in simple domains shown in Appendix D.1). DDL’s poor performance may be attributed to the absence of guiding signals and the instability of the reward function. Pairwise comparison guidance makes it difficult for PEBBLE to complete subgoal. HER, a classic GCRL algorithm, serves as a benchmark for evaluating other algorithms. Yet, HhP, despite integrating human guidance and curiosity-driven exploration, underperforms compared to HER in FetchPush. Its benefits are also unclear in Pusher and Four Rooms. This indicates HhP’s inadequate use of human guidance and curiosity in exploration. In contrast, MENTOR, by incorporating Dynamic Distance Constraint and Exploration-Exploitation Decoupling, effectively leverages these elements for exploration, achieving faster and more consistent training than DDL, PEBBLE, and HER. Our analysis highlights the superior performance of MENTOR.

5.3 ANALYZING THE INFLUENCE OF DYNAMIC DISTANCE CONSTRAINT (RQ2)

Our study will examine DDC’s effects on learning agents, assessing its impact on agent behaviors and the efficiency

of its auto-balancing coefficient for algorithm convergence. We also explore DDC’s synergism with human feedback.

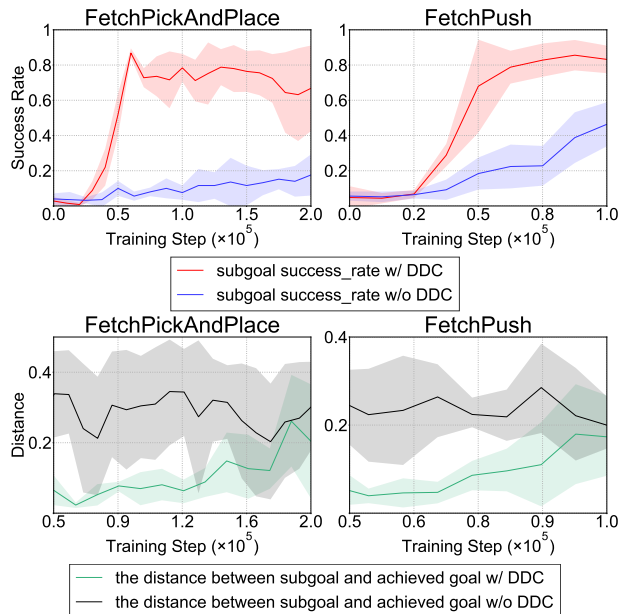


Figure 5: Impacts of Distance Constraints on success rate in FetchPickAndPlace and FetchPush domains. Since the high-level policy requires data to be collected before updating, a segment is missing from the distance curve.

Examining the correlation between task completion and DDC. As illustrated in Figure 5, when comparing the black and green curves on the lower side, It is evident that DDC

can regulate the difficulty of subgoals provided by limiting the distance. Without DDC, the high-level policy proposes subgoals at random difficulty. By examining this phenomenon in conjunction with the success rate of the subgoals, we can draw the following conclusions: (1) during the initial stages of the training process, the low-level policy can rapidly acquire the ability to achieve easy subgoals. (2) Once the low-level policy has successfully mastered a subgoal of a certain difficulty level, it can efficiently progress to learning subgoals of slightly higher difficulty. When there is no DDC, subgoals of randomized difficulty lead to slower learning of the low-level policy. It is concluded that the DDC can efficiently coordinate high-level and low-level.

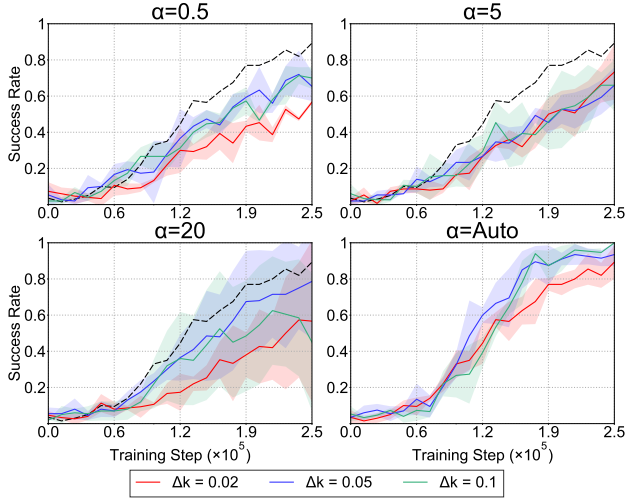


Figure 6: Effects of the balancing coefficient on the environment goal success rate in FetchPickAndPlace domains are examined on five random seeds. In the first three graphs, the dashed lines represent the average success rate with auto-set α in the worst case, where Δk is 0.02. The adjustment value of k is represented as Δk . We modify the parameter k to increase on successful completion of the subgoal and decrease on failure.

Analyzing the impact of automatic balancing coefficient.

DDC has a mechanism to automatically adjust the balancing coefficient. The mechanism plays a crucial role in balancing the impact of the reward model and distance constraint. As shown in Figure 6, fixed values of 0.5, 5, and 20 for α are ineffective in learning compared to the automatic adjustment setting. Small alpha values (0.5 and 5) slow DDC convergence. Large alpha (20) enhances learning speed but makes it unstable and sensitive to Δk . The auto-adjusted α mechanism converges rapidly and doesn't demand any fine-tuning for Δk .

Analyzing the overlay effects of DDC and human feedback. Having investigated DDC's impact, we now turn to assess the combined influence of human guidance and DDC on subgoal formulation. Figure 7 depicts the training phase

subgoal distribution, both with and without DDC. To the right of the figure, DDC's inactivity results in a fragmented learning interaction between levels. While the high-level, aided by human guidance, swiftly navigates to the goal, it neglects the low-level's execution capabilities, leading to transient and inefficient guidance, evident in the predominance of red subgoals in most regions except the upper-right corner. In contrast, on the figure's left, with DDC active, the high-level delineates a subgoal sequence starting from the lower right, proceeding to the lower left, then the upper left, and culminating at the upper right corner. This strategy, different from the scenario without DDC, significantly bolsters the efficiency of human guidance, contributing to MENTOR overall effectiveness. We also analyze the heatmap of reward and distance model, presented in Appendix D.2.

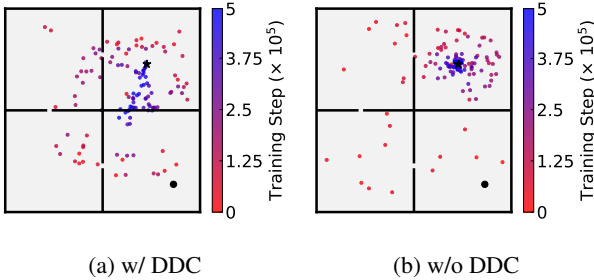


Figure 7: In Four rooms domain, we compare subgoal distributions with and without DDC during training. Subgoals are shown as colored circles, with a red-to-blue gradient for training time. The starting point is marked by a black circle in the lower right, while the ending point is a pentagram in the upper left.

5.4 ANALYZING THE IMPACT OF HUMAN FEEDBACK (RQ3)

Table 1: Cross-analysis on episodes (100 steps per episode) to the success of variables batch queries and query frequency. For each combination of variables, we ran 5 trials on different seeds and recorded the mean and variance.

Batch Queries	Query Frequency		
	25	50	100
0	3522±1441	-	-
10	1565±128	1765±268	1820±261
25	1455±165	1770±108	1683±203
50	1406±55	1735±253	1760±277

Analyzing the quantity and frequency of feedback. In Table 1, the data shows the number of training episodes needed for 100% task success across different query frequencies and batch sizes. The table illustrates that integrating human feedback into training markedly improves learning speed, as

highlighted by the contrast between label-free experiments and those with feedback. Further analysis demonstrates a consistent pattern: higher feedback frequency and quantity correlate with increased success rates. When considering the total labels and their impact on learning speed, our algorithm significantly enhances efficiency and stability by requiring only a small number of labels: 10 per 100 episodes, totaling 180, compared to experiments with non-feedback.

Comparing human collected labels and synthetic labels. In our study, we employ two methods for providing human guidance: synthetic labels generated through scripted techniques and human-generated labels. As explained in Figure 8, models trained with human labels exhibited comparable learning rates, with performance differences potentially attributed to noise in human feedback. Comparing experiments with human feedback to those without any guidance suggests that real human feedback is effective for policy training.

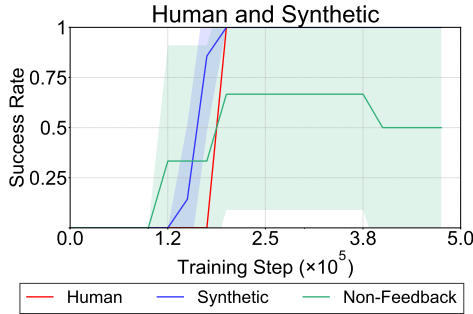


Figure 8: Experiments for evaluating MENTOR with script-generated and human-collected labels on the Four rooms domain given 10 labels every 25 episodes. Script-generated labels and non-feedback experiments are based on five random seeds, and the human-collected label experiment is based on one random seed.

5.5 ABLATION STUDIES (RQ4)

The ablation study in the MENTOR framework, focusing on the FetchPickAndPlace and FetchPush domains, evaluates how components like HF (human feedback), DDC, and EED (Exploration-Exploitation Decoupling) contribute to learning efficiency and goal achievement. Figure 9 (top) assesses each module’s effectiveness by systematically removing high-level modules and observing the impact on model performance. The removal of DDC and human feedback results in slower convergence, reduced performance, and decreased stability. The study mentioned in Figure 9 (bottom) discovered that the absence of EED negatively affects the balance between exploration and exploitation, resulting in lower success rates even after algorithm convergence. This emphasizes the significance and interdependence of these modules in improving learning for complex tasks in the MENTOR

framework.

In addition to DDC and EED, we employ various techniques such as near-policy sampling in RLHF, and negative sampling in distance model learning and explore encouragement in high-level policy. These ablation studies are presented in Appendix D.3.

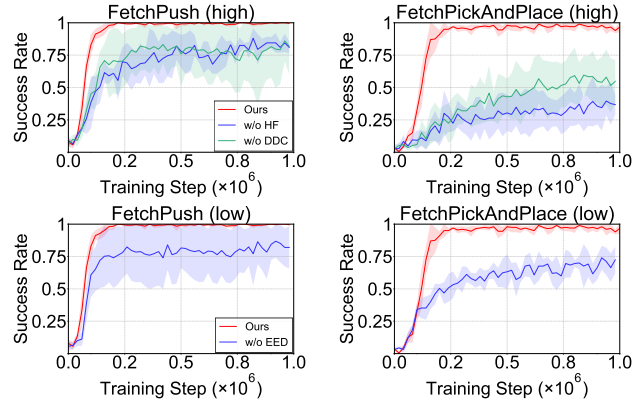


Figure 9: Ablations studies for MENTOR in FetchPickAndPlace and FetchPush domains at five random seeds. The ablation experiment involved immobilizing the low-level policy, removing the HF and DDC functions of the high-level policy, immobilizing the high-level policy, and removing the EED at the low-level.

6 CONCLUSION

This study presents MENTOR, an innovative method that combines human feedback and Dynamic Distance Constraint for learning guidance. It integrates high-level human insights for selecting subgoals concerning low-level capabilities and introduces exploration-exploitation decoupling at the low-level to improve training stability and efficiency. Our experiments demonstrate the framework’s effectiveness in complex tasks with sparse rewards, outperforming existing baselines.

However, we recognize the complexity of human guidance beyond just subgoal selection and aim to explore a wider range of feedback integration to enhance learning dynamics. We plan to further expand the framework’s applications and refine its mechanisms, aiming to advance hierarchical reinforcement learning and create more intuitive, adaptable learning systems.

references

Michael Ahn, Anthony Brohan, Noah Brown, Yevgen Chebotar, Omar Cortes, Byron David, Chelsea Finn, Chuyuan Fu, Keerthana Gopalakrishnan, Karol Hausman, et al.

- Do as i can, not as i say: Grounding language in robotic affordances. *arXiv preprint arXiv:2204.01691*, 2022.
- Marcin Andrychowicz, Filip Wolski, Alex Ray, Jonas Schneider, Rachel Fong, Peter Welinder, Bob McGrew, Josh Tobin, OpenAI Pieter Abbeel, and Wojciech Zaremba. Hindsight experience replay. *Advances in neural information processing systems*, 30, 2017.
- Pierre-Luc Bacon, Jean Harb, and Doina Precup. The option-critic architecture. In *Proceedings of the AAAI conference on artificial intelligence*, volume 31, 2017.
- Akhil Bagaria and George Konidaris. Option discovery using deep skill chaining. In *International Conference on Learning Representations*, 2019.
- Marc Bellemare, Sriram Srinivasan, Georg Ostrovski, Tom Schaul, David Saxton, and Remi Munos. Unifying count-based exploration and intrinsic motivation. *Advances in neural information processing systems*, 29, 2016.
- Nicolas Bougie and Ryutaro Ichise. Hierarchical learning from human preferences and curiosity. *Applied Intelligence*, pages 1–21, 2022.
- Ralph Allan Bradley and Milton E Terry. Rank analysis of incomplete block designs: I. the method of paired comparisons. *Biometrika*, 39(3/4):324–345, 1952.
- Tom Brown, Benjamin Mann, Nick Ryder, Melanie Subbiah, Jared D Kaplan, Prafulla Dhariwal, Arvind Neelakantan, Pranav Shyam, Girish Sastry, Amanda Askell, et al. Language models are few-shot learners. *Advances in neural information processing systems*, 33:1877–1901, 2020.
- Yuri Burda, Harrison Edwards, Amos Storkey, and Oleg Klimov. Exploration by random network distillation. *arXiv preprint arXiv:1810.12894*, 2018.
- Víctor Campos, Alexander Trott, Caiming Xiong, Richard Socher, Xavier Giró-i Nieto, and Jordi Torres. Explore, discover and learn: Unsupervised discovery of state-covering skills. In *International Conference on Machine Learning*, pages 1317–1327. PMLR, 2020.
- Thomas G Dietterich. Hierarchical reinforcement learning with the maxq value function decomposition. *Journal of artificial intelligence research*, 13:227–303, 2000.
- Benjamin Eysenbach, Abhishek Gupta, Julian Ibarz, and Sergey Levine. Diversity is all you need: Learning skills without a reward function. *arXiv preprint arXiv:1802.06070*, 2018.
- Dibya Ghosh, Abhishek Gupta, Justin Fu, Ashwin Reddy, Coline Devin, Benjamin Eysenbach, and Sergey Levine. Learning to reach goals without reinforcement learning. 2019.
- Jean Harb, Pierre-Luc Bacon, Martin Klissarov, and Doina Precup. When waiting is not an option: Learning options with a deliberation cost. In *Proceedings of the AAAI Conference on Artificial Intelligence*, volume 32, 2018.
- Kristian Hartikainen, Xinyang Geng, Tuomas Haarnoja, and Sergey Levine. Dynamical distance learning for semi-supervised and unsupervised skill discovery. *arXiv preprint arXiv:1907.08225*, 2019.
- Matthias Hutsebaut-Buysse, Kevin Mets, and Steven Latré. Hierarchical reinforcement learning: A survey and open research challenges. *Machine Learning and Knowledge Extraction*, 4(1):172–221, 2022.
- Yuu Jinnai, David Abel, David Hershkowitz, Michael Littman, and George Konidaris. Finding options that minimize planning time. In *International Conference on Machine Learning*, pages 3120–3129. PMLR, 2019.
- Kimin Lee, Laura Smith, and Pieter Abbeel. Pebble: Feedback-efficient interactive reinforcement learning via relabeling experience and unsupervised pre-training. *arXiv preprint arXiv:2106.05091*, 2021a.
- Kimin Lee, Laura Smith, Anca Dragan, and Pieter Abbeel. B-pref: Benchmarking preference-based reinforcement learning. *arXiv preprint arXiv:2111.03026*, 2021b.
- Andrew Levy, George Konidaris, Robert Platt, and Kate Saenko. Learning multi-level hierarchies with hindsight. *arXiv preprint arXiv:1712.00948*, 2017.
- Yongle Luo, Yuxin Wang, Kun Dong, Qiang Zhang, Erkang Cheng, Zhiyong Sun, and Bo Song. Relay hindsight experience replay: Self-guided continual reinforcement learning for sequential object manipulation tasks with sparse rewards. *Neurocomputing*, 557:126620, 2023.
- Jincheng Mei, Chenjun Xiao, Csaba Szepesvari, and Dale Schuurmans. On the global convergence rates of softmax policy gradient methods. In *International Conference on Machine Learning*, pages 6820–6829. PMLR, 2020.
- Ofir Nachum, Shixiang Shane Gu, Honglak Lee, and Sergey Levine. Data-efficient hierarchical reinforcement learning. *Advances in neural information processing systems*, 31, 2018.
- Long Ouyang, Jeffrey Wu, Xu Jiang, Diogo Almeida, Carroll Wainwright, Pamela Mishkin, Chong Zhang, Sandhini Agarwal, Katarina Slama, Alex Ray, et al. Training language models to follow instructions with human feedback. *Advances in Neural Information Processing Systems*, 35:27730–27744, 2022.
- Jongjin Park, Younggyo Seo, Jinwoo Shin, Honglak Lee, Pieter Abbeel, and Kimin Lee. Surf: Semi-supervised reward learning with data augmentation for feedback-efficient preference-based reinforcement learning. *arXiv preprint arXiv:2203.10050*, 2022.

- Seohong Park, Kimin Lee, Youngwoon Lee, and Pieter Abbeel. Controllability-aware unsupervised skill discovery. *arXiv preprint arXiv:2302.05103*, 2023.
- Ronald Parr and Stuart Russell. Reinforcement learning with hierarchies of machines. *Advances in neural information processing systems*, 10, 1997.
- Deepak Pathak, Pulkit Agrawal, Alexei A Efros, and Trevor Darrell. Curiosity-driven exploration by self-supervised prediction. In *International conference on machine learning*, pages 2778–2787. PMLR, 2017.
- Matthias Plappert, Marcin Andrychowicz, Alex Ray, Bob McGrew, Bowen Baker, Glenn Powell, Jonas Schneider, Josh Tobin, Maciek Chociej, Peter Welinder, et al. Multi-goal reinforcement learning: Challenging robotics environments and request for research. *arXiv preprint arXiv:1802.09464*, 2018.
- Siddharth Reddy, Anca D Dragan, and Sergey Levine. Sqil: Imitation learning via reinforcement learning with sparse rewards. *arXiv preprint arXiv:1905.11108*, 2019.
- Aadirupa Saha and Akshay Krishnamurthy. Efficient and optimal algorithms for contextual dueling bandits under realizability. In *International Conference on Algorithmic Learning Theory*, pages 968–994. PMLR, 2022.
- Tom Schaul, Daniel Horgan, Karol Gregor, and David Silver. Universal value function approximators. In *International conference on machine learning*, pages 1312–1320. PMLR, 2015.
- Nihar B Shah, Sivaraman Balakrishnan, Joseph Bradley, Abhay Parekh, Kannan Ramch, Martin J Wainwright, et al. Estimation from pairwise comparisons: Sharp minimax bounds with topology dependence. *Journal of Machine Learning Research*, 17(58):1–47, 2016.
- Archit Sharma, Shixiang Gu, Sergey Levine, Vikash Kumar, and Karol Hausman. Dynamics-aware unsupervised discovery of skills. *arXiv preprint arXiv:1907.01657*, 2019.
- Mel Vecerik, Todd Hester, Jonathan Scholz, Fumin Wang, Olivier Pietquin, Bilal Piot, Nicolas Heess, Thomas Rothörl, Thomas Lampe, and Martin Riedmiller. Leveraging demonstrations for deep reinforcement learning on robotics problems with sparse rewards. *arXiv preprint arXiv:1707.08817*, 2017.
- Tianren Zhang, Shangqi Guo, Tian Tan, Xiaolin Hu, and Feng Chen. Adjacency constraint for efficient hierarchical reinforcement learning. *IEEE Transactions on Pattern Analysis and Machine Intelligence*, 45(4):4152–4166, 2022.

A MENTOR DETAILS

A.1 EXECUTE PROCESS

In this section, we will comprehensively explain our framework MENTOR using pseudo-code in Algorithm 1. During the interaction with the environment (from line 5 to line 18), a high-level policy, referred to as π_{hi} , is responsible for selecting a subgoal sg (line 7). Once the subgoal is determined, a low-level explore policy, denoted as π_{lo}^e , is utilized to execute actions until the subgoal is successfully achieved. This process of selecting subgoals and executing actions continues until the end of the episode. The data obtained from the interaction with the environment, both at the high-level and low-level, is stored in two replay buffers known as B_{hi} and B_{lo} . The model update process is implemented in lines 20 to 24. The high-level policy in Algorithm 3 updates π_{hi} and α alternately, following equations 9 and 10. As for the low-level policy, it involves updating the RND model, applying hindsight, updating the low-level base policy π_{lo} , adding the RND bonus in the batch data, and updating the explore policy π_{lo}^e . From line 22 to 23, preference tuple pairs are sampled from the data of the last few episodes in B_{hi} and human labels are obtained and stored in B_{hf} . These batches are then used to update r_{hf} and rewrite the reward data in the high-level buffer B_{hi} . Finally, distance training data is sampled from the data of the last few episodes in B_{hi} and used to update the distance model d . From line 27 to 35, it tests the low-level base policy success rate on the subgoal sg given by high-level policy and adjusts the hyper-parameters k .

$$\theta_{hi} = \theta_{hi} + \eta_{\pi} \mathbb{E}_{\theta} [\nabla_{\theta} \log \pi(s, sg, g) (\sum r_{hi}(s, sg, g) - \alpha H(sg, g, k))] \Big|_{\substack{\theta = \theta_{hi} \\ \pi = \pi_{hi}}} \quad (9)$$

$$\alpha = \alpha - \eta_{\alpha} \nabla_{\alpha} \mathbb{E} [-\alpha (d(sg, g) - k)] \Big|_{\alpha = \alpha} \quad (10)$$

Algorithm 2 TrainHighPolicy

- 1: **Input:** high-level base policy π_{hi} , distance model d , balancing coefficient α , high-level buffer B_{hi}
 - 2:
 - 3: **for** $i = 0$ to N_2 **do**
 - 4: sample a batch B from buffer B_{lo}
 - 5: use batch B to update policy π_{hi} using Equation (9)
 - 6: use batch B to dual variable α using Equation (10)
 - 7: **end for**
-

Algorithm 3 TrainLowPolicy

- 1: **Input:** low-level base policy π_{lo} , low-level explore policy π_{lo}^e , RND model f_{rnd} , low-level buffer B_{lo}
 - 2:
 - 3: **for** $i = 0$ to N_3 **do**
 - 4: sample a batch B from buffer B_{lo}
 - 5: use batch B to update RND model f_{rnd}
 - 6: using hindsight to rewrite the goal and reward using r_g in B
 - 7: use batch B to update policy π_{lo}
 - 8: add RND bonus f_{rnd} to reward in B
 - 9: use batch B to update explore policy π_{lo}^e
 - 10: **end for**
-

B DOMAINS DETAILS

In this section, we will provide further elaboration on the benchmarks utilized for comparing our method with the baselines. Specifically, we will delve into the details of the observation space, action space, and the configuration of the reward function.

FetchPush. In this domain, the aim is to use a 7-DoF Fetch Mobile Manipulator, equipped with a closed two-fingered parallel gripper, for transporting a block to a set position on a table. The robot’s movement is finely adjusted using Cartesian coordinates, and the MuJoCo framework calculates the inverse kinematics. This task, which involves pushing the block with the gripper constantly closed, is ongoing, requiring the robot to steadily keep the block at the target position. The scenario is observed through a 25-element array, encompassing kinematic details of both the block and gripper. The action space is a `Box(-1.0, 1.0, 4, float32)`, with each action altering the gripper’s Cartesian position (dx , dy , dz) and managing its opening and closing. The reward system applies -1 when the block isn’t at the target, and 0 when correctly positioned, defined as being within 0.05 meters of the target.

Algorithm 1 MENTOR: High-level Adaptive Control with Dynamic Distance Constraints

```
1: Input: initial state distribution  $\rho(s)$ , goal distribution  $\rho(g)$ 
2: Initialize high-level policy  $\pi_{hi}$ , low-level base policy  $\pi_{lo}$ , low-level explore policy  $\pi_{lo}^e$ , reward model  $r_{hf}$ , RND model  $f_{rnd}$ , distance model  $d$ , balancing coefficient  $\alpha$ , constraint hyper-parameters  $k$ , high-level buffer  $B_{hi}$ , preference buffer  $B_{hf}$  and low-level buffer  $B_{lo}$ .
3:
4: for  $i = 0$  to  $M$  do
5:   receive initial state  $s_t$  and initial  $g$  from the environment,  $s_t \leftarrow \rho(s), g \leftarrow \rho(g)$ 
6:   repeat
7:     select a subgoal  $sg \leftarrow \pi_{hi}(s_t, g)$ 
8:     store high-level state  $s_{hi} \leftarrow s_t$ 
9:     repeat
10:      select action  $a_t \leftarrow \pi_{lo}^e(s_t, sg)$ 
11:      execute  $a_t$  and observe next state  $s_{t+1}$ 
12:      compute low-level reward  $r_{lo} = r_g(s_{t+1}, sg)$ 
13:      store  $(s_t, a_t, s_{t+1}, sg, r_l)$  to low-level buffer  $B_{lo}$ 
14:       $s_t \leftarrow s_{t+1}$ 
15:    until  $terminal(s_t, sg)$ 
16:    calculate the high reward  $r_{hi} \leftarrow r_{hf}(s_{hi}, g, sg)$ 
17:    append  $(s_{hi}, sg, s_t, g, r_{hi})$  to  $B_{hi}$ 
18:     $s_{hi} \leftarrow s_t$ 
19:  until end of episode
20:  TrainHighPolicy( $\pi_{hi}, f_{rnd}, d, \alpha, B_{hi}$ ) Algorithm 2
21:  TrainLowPolicy( $\pi_{lo}, \pi_{lo}^e, f_{rnd}, B_{lo}$ ) Algorithm 3
22:  near policy query preference tuples pairs from  $B_{hi}$  and store preferences in  $B_{hf}$ 
23:  update  $r_{hf}$  on batches from  $B_{hf}$  and rewrite the reward in  $B_{hi}$ 
24:  near policy sample distance batches from  $B_{lo}$  and update distance model  $d$  using Equation (4)
25:   $success\_rate \leftarrow \{\}$ 
26:  for  $j = 0$  to  $N_1$  do
27:    sample goal  $g$  from environment and select a subgoal  $sg$ 
28:    execute actions using low-level base policy  $\pi_{lo}$  on subgoal  $sg$  and store the success state in  $success\_rate$ 
29:  end for
30:  if  $average(success\_rate) \geq high\_threshold$  then
31:    increase  $k$  value
32:  end if
33:  if  $average(success\_rate) < low\_threshold$  then
34:    decrease  $k$  value
35:  end if
36: end for
```

FetchPickAndPlace. Utilizing the same robot setup with FetchPush, this domain focuses on moving a block to a defined point, including mid-air locations. It shares the same observation array and action space as FetchPush, with the addition of a goal-aware observation space. The reward system remains consistent with the FetchPush domain.

FetchDraw. Utilizing the same 7-DoF Fetch Mobile Manipulator with a two-fingered parallel gripper, this task involves the robot’s precise interaction with a drawer. The objective is two-fold: (1) to reach for the drawer handle, and (2) to slide the drawer to a target position by pulling or pushing the handle. The manipulation requires the gripper to perform open and close actions for a firm grasp on the drawer handle. The robot must successfully move and maintain the drawer at the target position indefinitely. The reward system remains consistent with the FetchPush domain.

FetchObsPush. This task engages the same 7-DoF Fetch Mobile Manipulator, which is equipped with a two-fingered parallel gripper. The robot is tasked with manipulating a block to a desired position on a table in the presence of an obstacle. The challenge requires the robot to (1) approach and securely grasp the block, and (2) navigate and push the block to the target location, accounting for the obstacle whose size and shape are unknown. This task demands precision handling and adaptability to avoid obstacle while ensuring the block reaches its target position. As with the FetchPush, FetchObsPush is continuous, with the robot required to keep the block within 0.05 meters of the target position indefinitely. The reward system remains consistent with the FetchPush domain.

Pusher. This domain involves the manipulation of a robotic arm, specifically a sawyer robotic arm, in an environment with multiple obstacles. The objective is to successfully push an obstacle, referred to as a puck, to a designated goal area marked by a red dot. Unlike the FetchPush problem, which has a 25-dimensional observation, the state space in this environment is determined by the position of the puck and the arm. The action space, on the other hand, involves controlling the position of the robotic arm. It is a discrete 9-dimensional space where each action corresponds to a delta change in the position in a 2-D space. The reward system remains consistent with the FetchPush domain.

Four rooms. In the four-room domain, the agent’s task is to navigate to a specified goal while dealing with initially unknown obstacles. The agent is positioned at (0.4, -0.4) in the bottom right room, aiming for the goal at (0.25, 0.25) in the top right room. The state observation is the agent’s precise (x, y) location, and it has a set of 9 possible actions to choose from, which allow movement in all cardinal and diagonal directions, or to remain stationary. Key to this task are the doorways in the walls, which are the sole means for the agent to traverse between rooms.

In the FetchPush, FetchPickAndPlace, FetchDraw, FetchObsPush, and Pusher domains, synthetic labels are generated using a dense sparse approach. This means that the reward returned is calculated as the negative Euclidean distance between the achieved goal position and the desired goal. In the Four rooms domain, we utilize the reward function displayed in Equation (11). The reward heatmap, referred to as the oracle reward model, is depicted in Figure 11. In the top right quadrant, the agent receives a reward based on the negative Euclidean distance from its current position s to the goal $[0.25, 0.25]$. In the top left quadrant, the reward is the negative Euclidean distance from s to a fixed point $[0, 0.3]$, with an additional penalty of -0.3. In the bottom left quadrant, the reward is the negative Euclidean distance from s to $[-0.3, 0]$, with a penalty of -0.6. In the bottom right quadrant, it is the negative Euclidean distance from s to $[0, -0.3]$, with a penalty of -1.

$$\Gamma_{\text{Four rooms}}(s) = \begin{cases} -\|s - [0.25, 0.25]\|_2 & \text{if } s_x \geq 0 \text{ and } s_y \geq 0 \\ -\|s - [0, 0.3]\|_2 - 0.3 & \text{if } s_x \leq 0 \text{ and } s_y \geq 0 \\ -\|s - [-0.3, 0]\|_2 - 0.6 & \text{if } s_x \leq 0 \text{ and } s_y \leq 0 \\ -\|s - [0, -0.3]\|_2 - 1 & \text{if } s_x \geq 0 \text{ and } s_y \leq 0 \end{cases} \quad (11)$$

C IMPLEMENTATION DETAILS

In this section, we will present the implementation details of each baseline used in our experiments. We will also discuss the reasonable and necessary modifications made to the original algorithm, as well as provide the rationale behind these modifications.

C.1 MENTOR

The executing process details of MENTOR is introduced in Appendix A. Here, we only provide the hyperparameters.

Table 2: Hyperparameters of MENTOR.

Hyperparameters	Values
High-level policy	
Actor learning rate	3×10^{-4}
Critic learning rate	3×10^{-4}
Replay buffer size	10^6
Hidden layers	3
Hidden size	256
Batch size	256
Soft update rate	0.005
Policy update frequency	1
γ	0.99
Distance model learning rate	3×10^{-4}
Distance model replay buffer size	1000
Distance model hidden layers	3
Distance model hidden size	256
Distance model batch size	256
Reward model learning rate	3×10^{-4}
Reward model replay buffer size	1000
Reward model hidden layers	3
Reward model hidden size	256
Reward model batch size	256
success rate high threshold	0.6
success rate low threshold	0.3
Δk	0.05
Low-level policy	
Actor learning rate	10^{-3}
Critic learning rate	10^{-3}
Hidden layers	3
Hidden size	256
Replay buffer size	10^6
Batch size	512
Soft update rate	0.005
Policy update frequency	1
γ	0.95
RND learning rate	3×10^{-4}
RND hidden layers	3
RND hidden size	256
RND represent size	512
RND bonus scaling	1.0
Hindsight sample ratio	0.8

C.2 HhP

HhP introduces a HRL method that integrates human preferences and curiosity-driven exploration. By using human preferences to guide decision-making at high-levels and curiosity to promote environmental exploration at low-levels. HhP is considered to be inefficient in combining HRL and RLHF, and it also introduces bias at the low-levels. When we trained HhP, we found that this algorithm was difficult to converge, and to ensure the effectiveness of training, we introduced the hindsight technique in this algorithm as well.

C.3 HER

HER enables efficient learning from limited and non-diverse rewards by re-framing failed attempts as successes towards different goals. In our implementation, we utilize a 3-layer MLP policy to incorporate HER. When sampling batch transitions from the replay buffer, we employ hindsight technology to modify certain parts of the transitions. It is important to mention that the high-level policy differs from the low-level policy of MENTOR in certain aspects. Unlike the low-level policy, the high-level policy solely receives goals from the environment and does not incorporate an RND bonus.

C.4 DDL

DDL (dynamic distance learning) calculates dynamical distances, defining them as the expected number of steps between states in a system. This method leverages unsupervised interactions for learning distances. In the distance evaluation step, the aim is to estimate the dynamical distance between pairs of states visited by a given policy. A distance function, denoted as $d(s_i, s_j)$, is utilized for this purpose. To calculate the distance, multiple trajectories, denoted as τ , are generated by rolling out the policy. Each trajectory has a length of T . The empirical distance between states s_i and s_j in the trajectory τ is then calculated, where $0 \leq i \leq j \leq T$. The empirical distance is simply given by the difference between j and i . To learn the distance function, supervised regression can be employed by minimizing the objective.

$$\mathcal{L}_d = \frac{1}{2} \mathbb{E}_{\tau \sim p_\tau} \left[\sum_{i \in [0, T]} \sum_{j \in [i, T]} (d_\psi(s_i, s_j) - (j - i))^2 \right]. \quad (12)$$

To address the GCRL problem, it is crucial to incorporate negative samples to enhance the distance between states and goals that cannot be attained solely through a low-level policy. Additionally, we adopt the objective defined in Equation (4).

C.5 PEBBLE

The key concept of PEBBLE is to learn a reward model on human preference. Unlike the learning strategy of the REWARD model in the MENTOR, it has an unsupervised pretraining step via intrinsic reward. Here, we apply the state entropy $H(s) = -\mathbb{E} \log p(s)$. By converting the policy to a simpler version, the pretraining reward function is set as $\log(\|s_i - s_i^k\|)$ in the batch. This implies that maximizing the distance between a state and its nearest neighbor increases the overall state entropy.

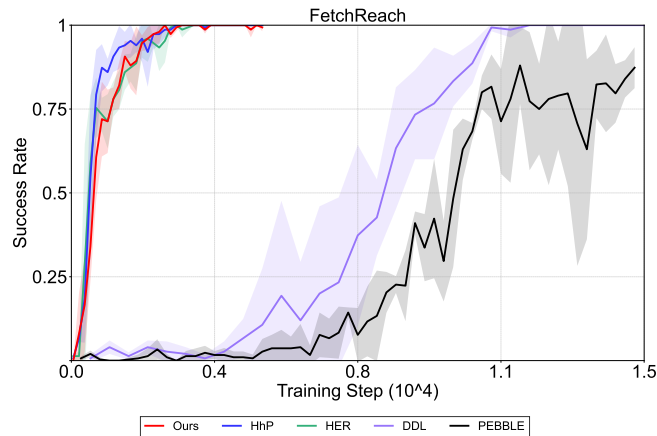


Figure 10: Experiments on easy domain FetchReach. DDL and PEBBLE successfully learned the task in FetchReach.

D FURTHER ANALYSIS AND ABLATIONS

In this section, we will provide analysis and additional ablations not included in the main body.

D.1 EXPERIMENTS ON FETCHREACH

As demonstrated in Figure 4, the findings indicate that DDL and PEBBLE exhibit limited effectiveness in complex GCRL domains. However, when these methods are employed in FetchReach, a domain that solely involves the movement of the fetch mobile manipulator to a specified point, there is a high likelihood that DDL and PEBBLE can complete this task within 15000 training steps in Figure 10. Other algorithms, such as MENTOR, HhP, and HER, can easily reach almost 100% success rate after 4000 training steps. These observations strongly indicate that DDL and human feedback based on pairwise comparison are not suitable approaches for solving the GCRL problem.

D.2 HEATMAP ANALYSIS OF ABLATED DDC

The analysis of the heatmaps in Figure 11 shows complex interactions between the distance and reward models in the MENTOR framework. On the right, the oracle reward function in the Four rooms domain indicates where the agent likely earns higher rewards, guiding it from the lower right to the upper right corner. On the left, the distance model assesses subgoal difficulty. The reward heatmap, shaped by human feedback, approximates the oracle function and overlaps with the distance heatmap. This overlap, calculated with $r_{hf}(s, sg, g) + \alpha H(sg, g, k)$, identifies areas optimizing rewards in alignment with the low-level policy’s capabilities. However, without DDC, the human feedback-based reward model is limited, indicating only high-reward areas without guiding the agent on how to reach them.

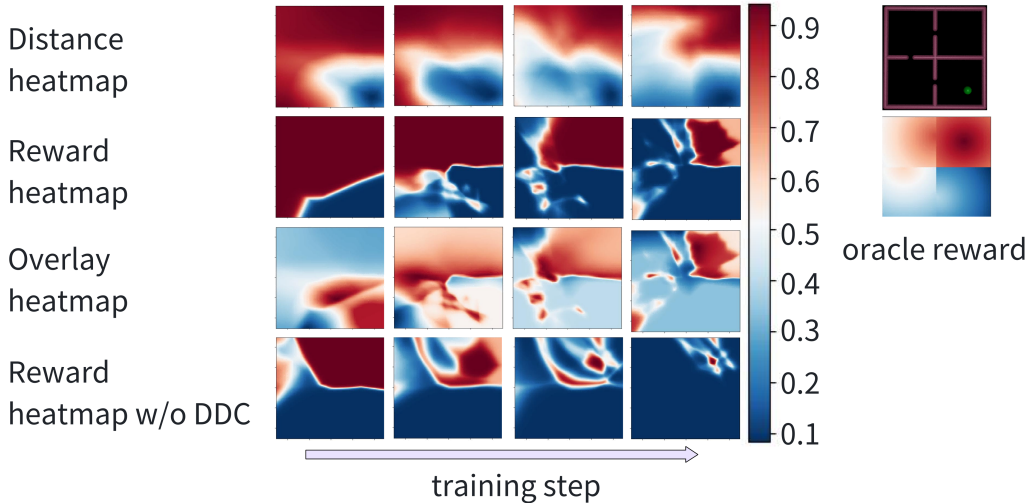


Figure 11: Evolutions of heatmaps on the Four rooms domain. The color scheme used in the heat map employs red to depict high values and blue to represent low values.

D.3 ABLATIONS OF NEGATIVE SAMPLING IN DDC, NEAR POLICY SAMPLING IN RLHF AND EXPLORATION AT THE HIGH-LEVEL

Tricks in RLHF and distance model. In Figure 12, we evaluate the effect of negative sampling in DDC and near policy sampling in RLHF. The distance heatmap without a negative sample gives an incorrect estimate of the distance from states to some subgoals that the low-level cannot reach. This error may induce the high-level policy to generate subgoals the low-level policy can not complete. The near policy is an additional technique in our framework. By comparing reward heatmaps with and without the inclusion of near-policy samples, we observe that when near-policy samples are absent, the reward model tends to emphasize the entirety of the state space. This, in turn, makes it more challenging and computing resource-consuming for the reward model to effectively learn.

Analysis exploration at the high-level. During the training process of MENTOR, we have observed that there are instances where the high-level policy becomes stuck in local optima as we incrementally increase the value of k for a long time. This phenomenon is attributed to two reasons: 1) It lacks pretraining at the high-level, and 2) the high-level lacks the exploratory ability, leading to not trying new subgoals. Pretraining plays a crucial role in RLHF, yet it can be inefficient at

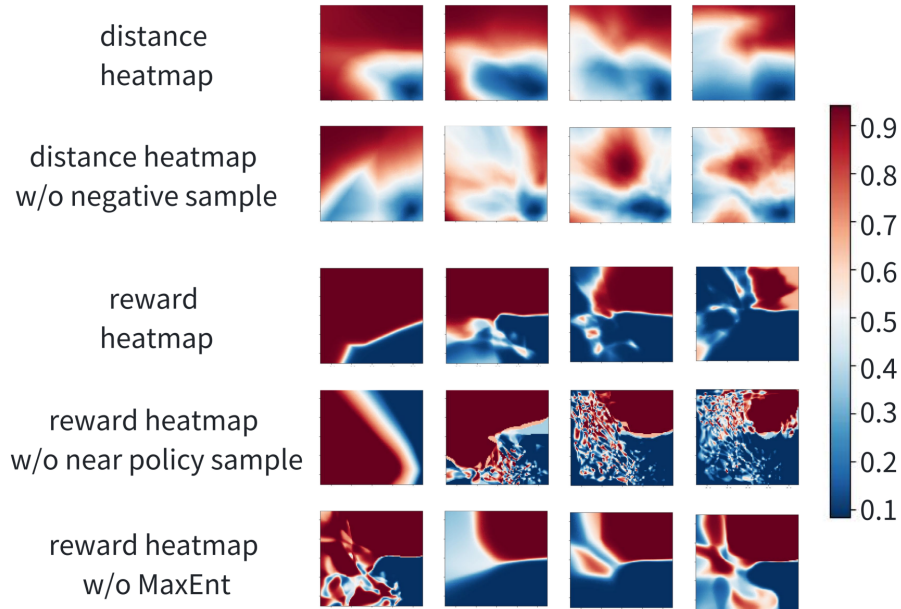


Figure 12: Further ablations

the high-level due to limited samples (often only one per episode). Sampling subgoals across the entire state space becomes computationally wasteful. Instead, the high-level policy does not require knowledge of the optimal subgoal’s location in the entire state space, but only within a specified distance range of k . When the high-level policy is optimized within a specified range of k , increasing k to $k + \Delta k$ results in the high-level policy getting stuck in local optima. This is because the reward model does not query new sample pairs to provide useful signals. In the operation of the high-levels, we find it necessary to increase the exploratory ability. As shown in Figure 12, reward learning becomes challenging without MaxEnt (maximum entropy). It gets stuck in the learned area and refuses to explore novel regions.

In addition, we compare RND and MaxEnt in terms of Exploratory at high-levels. After conducting experiments displayed in Figure 13, we discovered that MaxEnt outperforms RND. While RND promotes the exploration of novel states, MaxEnt focuses on improving action entropy. The combination of the reward model and DDC can lead to previously disregarded decisions being recognized as good decisions. RND can learn and incorporate these decisions previously, treating them as non-novel at late times. However, MaxEnt does not encounter this issue and as a result, it achieves significantly better performance compared to RND.

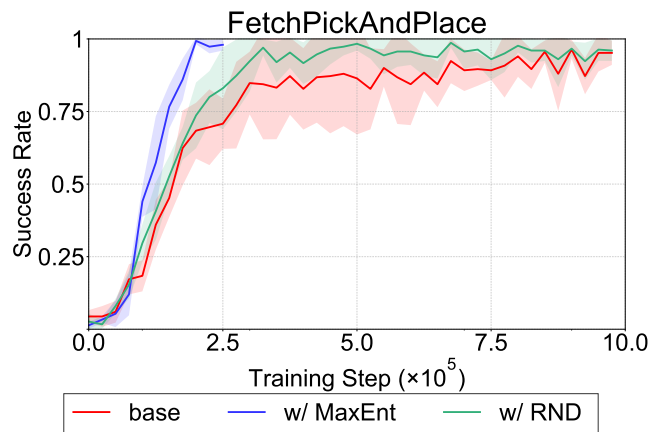


Figure 13: Explore encouragement effects analysis on FetchPickAndPlace domain.